Article

pubs.acs.org/Biomac

Green Nondegrading Approach to Alkyne-Functionalized Cellulose Fibers and Biohybrids Thereof: Synthesis and Mapping of the Derivatization

Gino Mangiante,[†,‡] Pierre Alcouffe,[†] Béatrice Burdin,[§] Marianne Gaborieau,[∥] Elisa Zeno,[‡] Michel Petit-Conil,[‡] Julien Bernard,[†] Aurélia Charlot,*[,†] and Etienne Fleury*[,†]

[†]Université de Lyon, F-69631, Lyon; INSA Lyon, F-69621, UMR CNRS 5223, Ingénierie des Matériaux Polymères F-69621, Villeurbanne, France

[§]Centre Technologique des Microstructures-CTμ, Université de Lyon, Villeurbanne, France

[∥]Nanoscale Organisation and Dynamics Group, School of Science and Health, University of Western Sydney, Parramatta campus, Locked bag 1797, Penrith NSW 2751, Australia

[‡]Centre Technique du Papier, Domaine Universitaire BP 251, 38044 Grenoble Cedex 9, France

Supporting Information

ABSTRACT: Alkyne-functionalized cellulose fibers have been generated through etherification under basic water or hydro-alcoholic conditions ($NaOH/H_2O$/isopropanol). For a given NaOH content, the medium of reaction and, more particularly, the water/IPA ratio, were shown to be of crucial importance to derivatize the fibers without altering their integrity and their crystalline nature. It was shown that the degree of substitution (DS) of the fibers increases concomitantly with isopropanol weight ratio and that, contrary to water or water-rich conditions, derivatization of fibers under isopropanol-rich conditions induces an alteration of the fibers. Optimization of etherification conditions in aqueous media afforded functionalized cellulose materials with DS up to 0.20. Raman confocal microscopy on derivatized fibers cross sections stressed that alkyne moieties are incorporated all over the fibers. The resulting fibers were postfunctionalized by molecular probes and macromolecules in aqueous or water-rich conditions. The effectiveness of the grafting was strongly impacted by the nature of the coupling agents.

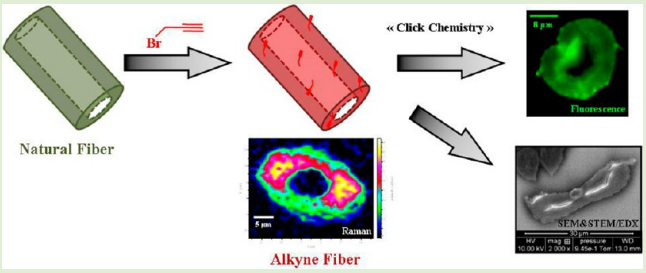

INTRODUCTION

In reaction to the rapid depletion of the Earth's finite fossil fuel reserves, our society currently has no choice but to develop energy and material technologies that rely on alternative, abundant, and renewable resources. In regard to materials science, the rational exploitation of biomass has regained significant interest lately. Cellulose, the most abundant polymer resource available today in the biosphere, logically appears as a key and inescapable actor of this forthcoming green technological transition and already finds numerous applications in areas such as composite materials, textiles, drug delivery systems, and personal care.[1] This polysaccharide, consisting of β-(1→4)-D-glucopyranosyl units, is essentially found in plant matter (wood, cotton, ...) in a fibrous state.[2] Wood cellulose fibers possess a hierarchical supramolecular structure with highly organized crystalline zones and amorphous regions.[3] This peculiar organization of the chains in cellulose fibers confers highly valuable features to cellulose materials in terms of mechanical properties, that is, tensile strength, Young modulus, and elongation at break.[4]

The availability and properties of cellulose fibers have encouraged numerous research groups to explore strategies affording the preparation of original biohybrid materials that combine the intrinsic features of the cellulosic fibers, that is, renewable and sustainable character, hydrophilicity, mechanical properties, and biodegradability with the attributes of synthetic polymers (tunable polarity, thermal stability, mechanical strength, antibacterial properties, responsive behavior, ...).[5] Numerous chemical routes have indeed been developed to precisely tune the (surface) properties of structured cellulose derivatives (fibers, microfibrils, cellulose nanocrystals) under heterogeneous conditions through covalent attachment of synthetic polymer chains using "grafting-onto", "grafting-through", or "grafting-from" approaches.[6] While a plethora of hybrid cellulose derivatives has been described over the past decade, the industrialization of such biohybrids has been hampered by the recurrent use during the grafting process of

Received: October 31, 2012
Revised: December 7, 2012
Published: December 10, 2012

dx.doi.org/10.1021/bm3016829 | Biomacromolecules 2013, 14, 254−263

industrially and environmentally unfriendly organic solvents and/or high temperatures that jeopardize the crystallinity and the inherent properties of the structured cellulose.

In the quest for green routes to cellulose-based biohybrids, the modification of cellulose materials in aqueous medium has recently been addressed. For instance, noncovalent strategies of cellulose derivatization have been described by Brumer and Teeri who exploited the tight association of xyloglucan, a polymer displaying a $\beta(1\rightarrow4)$-linked glucan backbone substituted by xylopyranosyl residues (bearing sometimes galactopyranosyl, fucopyranosyl, or arabinofuranosyl residues), and cellulose. The authors have reported on a series of xyloglucan polysaccharides carrying amine, fatty esters, thiol, haloester, and alkyne groups as well as xyloglucan-containing block copolymers to be bound to cellulose surfaces.[7] Laine and co-workers investigated the adsorption of aqueous solutions of carboxymethyl-cellulose bearing alkyne or azide functionalities onto various cellulose substrates (filter paper, regenerated cellulose surface, or whiskers-based surface).[8] While physical adsorption of natural or synthetic polymers is a promising route to confer desirable properties to cellulose substrates through a sustainable process, some functions and applications of biohybrids require the formation of stable covalent linkages between cellulose and the grafts. In this context, the establishment of green, efficient, and nondegrading procedures for the covalent introduction of synthetic segments onto cellulose fibers is therefore highly desirable.

In view of generating high-performance biohybrids in sustainable and industry-compatible conditions, alkyne-functionalized cellulose materials constitute very promising precursors because these functionalities are capable of rapidly reacting in aqueous medium under mild conditions with a large panel of functional groups such as thiols, alkynes, nitrile oxides, or azides.[9] Whereas significant efforts have been devoted to alkyne-functionalization of polysaccharides under homogeneous solutions (including destructured cellulose),[10] the introduction of alkyne groups on solid cellulose materials under heterogeneous conditions has not raised much attention thus far. Argyropoulos and co-workers reported on the grafting of alkyne groups on (TEMPO) oxidized cellulose nanocrystals through amidification and the preparation of nanoplatelet gels thereof.[11] Alkyne functionalization of cotton fibers through esterification in organic media at high temperatures was also recently examined separately by Haddleton and Halfrén.[12] Unfortunately, the impact of these processes on cellulose fiber integrity was not discussed in these contributions.

In this context, we explore herein the preparation of alkyne-functionalized wood cellulose fibers through Williamson etherification in conditions that are consistent with the concepts of sustainable chemistry, that is, aqueous or hydro-alcoholic medium (water/isopropanol), and that allow for substantial grafting yields while maintaining the integrity and the intrinsic properties of the fibers. In this article, we investigate in detail how the nature of the reaction medium together with other parameters such as the hydroxyl/propargyl bromide (PgBr) ratio or the duration of the reaction impact the etherification process and whether or not these conditions of alkynation alter the structure of the fibers. For a better understanding of the grafting process, we also report a precise mapping of the alkyne functionalization within the fibers through Raman confocal microscopy. Finally, the aqueous modification of the resulting alkyne-functionalized fibers through highly efficient ligation procedures and the spatial distribution of grafted entities (molecules and macromolecules) within the fibers are examined to evaluate the accessibility and the reactivity of the alkyne groups.

EXPERIMENTAL SECTION

Materials. The cellulose fibers (**1**) from bleached Kraft wood pulp were provided by CTP (Centre Technique du Papier, Grenoble) and were used as received. 2-Bromopropionic acid 3-azido-propyl ester (**4**) was prepared according to the method described by Quémener et al.[13] ω-N_3-Poly(ethylene glycol) (denoted ω-N_3-PEG; **8**) was synthesized following a protocol developed in our laboratory[14] from α-methoxy-ω-hydroxy-poly(ethylene glycol) purchased from Aldrich (M_n = 750 g·mol^{-1}). Azide-functionalized Alexa fluor 488 fluorescent probe (**6**) was supplied by Life Technologies. The other chemicals were purchased from Aldrich: propargyl bromide (PgBr; **2**; 80 wt % in toluene), sodium hydroxide (≥98%), (+)-sodium (L)-ascorbate (≥99%), and copper(II) sulfate (≥99%). The solvents were supplied by Carlo Erba.

Characterization of Raw and Chemically Modified Cellulose Fibers. *Solid-State NMR Spectroscopy.* Solid-state NMR experiments were performed on a Bruker DPX spectrometer operating at 200 MHz ^{1}H Larmor frequency with a commercial double resonance probe supporting zirconia MAS rotors with 4 mm outer diameter at a magic-angle spinning (MAS) frequency of 12 kHz. ^{1}H MAS spectra were recorded with a 78 kHz radiofrequency (RF) nutation frequency (4 μs 90° pulse length), 3 s relaxation delay, and 8 transients. ^{13}C cross-polarization (CP-MAS) spectra were recorded with a 89 kHz RF nutation frequency (3.5 μs 90° pulse length), 2 ms contact time, 5 s relaxation delay, and 2048−9216 transients. ^{13}C single pulse excitation (SPE-MAS) spectra were recorded with a 89 kHz RF nutation frequency (3.5 μs 90° pulse length), 5 s relaxation delay, and 18000−45000 transients. The ^{1}H and ^{13}C chemical shift scales were externally referenced to tetramethylsilane (TMS) at 0.0 ppm using adamantane by setting the CH resonances to 1.64 and 38.5 ppm, respectively.[15] The signal assignment was carried out by comparison with literature for cellulose[16] and poly(ethylene oxide).[17]

Raman Spectroscopy. Raman spectroscopy was carried out using a Kaiser RXN1 spectrometer equipped with an excitation wavelength of 785 nm and a beam power of 400 mW. Spectra were recorded on fibers inside a 5 mm NMR tube collecting between 200 and 3100 cm^{-1}.

Infrared (FT-IR) Spectroscopy. IR spectra were recorded with an IR Nicolet iS10 Thermo Scientific spectrometer collecting from 32 to 128 scans between 650 and 4000 cm^{-1}. Transmission was carried out using KBr pellets.

Elemental Analysis (EA). C, H, N, and O contents were obtained by classical CHN and O analysers based on pyrolysis and subsequent gas analysis. Br content was evaluated by combination of burning/ionic chromatography.

The degree of substitution (DS) in alkyne groups, that is, the average number of substituted cellulose hydroxyl groups per anhydroglucose unit (AGU), was determined from EA of 2-bromopropionic acid 3-azido-propyl-grafted fibers (**5**; vide infra) after confirmation of the quantitative character of the CuAAC (copper(I) catalyzed azide−alkyne cycloaddition) coupling between **3** and **4** (disappearance of the signal relative to alkyne groups evidenced by Raman spectroscopy). To evaluate accurately the DS and eliminate the contribution of physical adsorption of **4** on the fibers in the calculation of DS, "blank" samples, namely, alkyne-functionalized fibers (**3**) mixed with 2-bromopropionic acid 3-azido-propyl ester (**4**) without addition of catalyst were concomitantly analyzed.

Grafting of 2-bromopropionic acid 3-azido-propyl ester (**4**) on alkyne-functionalized fibers (**3**) was evaluated by the following eq I:

$$\mathrm{DS} = \frac{162.16}{236.09} \times \frac{\%_{N5}}{\%_{N4} - \%_{N5}} \qquad \text{(I)}$$

where $\%_{N4}$ and $\%_{N5}$ are, respectively, the amount of nitrogen in 2-bromopropionic acid 3-azido-propyl ester (**4**) and in the sample of

dx.doi.org/10.1021/bm3016829 | Biomacromolecules 2013, 14, 254−263

alkyne-functionalyzed fibers grafted with 2-bromopropionic acid 3-azido-propyl ester (**5**).

Grafting of ω-N_3-PEG (**8**) on alkyne-functionalized fibers (**3**) was evaluated by the following eq II:

$$DS_{PEG} = \frac{162.16}{775.08} \times \frac{\%_{N9}}{\%_{N8} - \%_{N9}} \quad \text{(II)}$$

where $\%_{N8}$ and $\%_{N9}$ are, respectively, the amount of nitrogen in ω-N_3-PEG (**8**) and in the sample of alkyne-functionalyzed fibers grafted with ω-N_3-PEG (**9**).

Characterization of the Functionalization Topology. *Preparation of Samples for Microscopy.* Raw or modified dried cellulose fibers were deposited on glass slide and washed with ethanol to remove residual traces of water. After evaporation of ethanol, the fibers were introduced in an embedding resin (Epofix) and the part was cured overnight at 55 °C. The resulting epoxy network was then cut with a Reichert ultracut E at room temperature to obtain thin slices of fiber cross sections. The slices were either deposited on or between two slides of glass (fluorescence, Raman confocal microscopies) or on a Formvar coated copper grid (EDX/STEM analyses).

Raman Confocal Microscopy. Raman confocal microscopy was performed out using a LabRam Image 1B spectrometer (Horiba Jobin-Yvon) with polarized 514 nm laser (10 mW) excitation, a CCD detector, and an Olympus BX40 microscope. The analyses were carried out with a 200 μm pinhole and a 100 μm slit aperture, 600 grooves/mm grating, and a 100× ON 0.9 objective lens. The 30 × 30 μm Raman micrographs were generated from spectral data using point-by-point scanning (900 scans/image) with a lateral resolution of 2 μm, a 2.1 μm optical slice, and a 15 cm^{-1} spectral resolution.

Fluorescence Confocal Microscopy. Fluorescence microscopy was performed using a confocal laser scanning microscope (Zeiss LSM510META) with a 488 nm excitation wavelength. The emission signal was collected between 505 and 530 nm. Micrographs were performed on slices of 0.8 μm with an apochromatic ×63/1.4NA objective lens. Fluorescence micrographs were recorded on a cross-section of Alexa Fluor 488 grafted fibers. To take adsorption phenomena into account, control samples, that is, alkyne-functionalized fibers treated in CuAAC conditions without addition of catalyst were also carried out. The settings of the emission source transmission power as well as the pinhole aperture, gain, and offset of the photomultiplier were accurately adjusted on the grafted fibers and maintained for the characterization of the control sample.

STEM/EDX. Scanning transmission electron microscopy (STEM) was performed on fiber cross-section using a JEOL 1200EX microscope at 80 kV. The EDX/STEM spectra were recorded on 0.25 μm^2 area during 100 s.

Crystalline/Morphological Characterizations. *XRD Measurements.* The fiber crystallinity was assessed by X-ray diffraction. A XRD Bruker D8 Advance diffractometer was utilized to scan and to record data, by using Cu Kα radiation at 2θ = 4.5−50° with a step size of 0.022° on a compacted fiber pellet.

Automated Optical Analysis. The microscopic dimensions of the fibers (mean length × diameter) were measured in water with a MorFi (TECHPAP) device developed by the Centre Technique du Papier (CTP, France) and the Ecole Française de Papeterie et des Industries Graphiques (EFPG, Grenoble, France). This ISO 16065−2:2007-certified instrument (determination of fiber length by automated optical analysis) determines the average diameter and length of fibers from dispersed fibers flow image processing. The values are the average of at least two measurements on wet fibers (without previous drying step), each one based on 15000 individual fibers analysis. The reported mean lengths are the mean length-weighted fiber lengths.

Synthesis. *Preparation of Alkyne-Functionalized Cellulose Fibers (**3**) in Hydroalcoholic Process (Example by Using H_2O/IPA, 70/30 (w/w), Reactions **12**−**14**).* Cellulose fibers (**1**; 3.00 g, 18.3 mmol anhydroglucose unit, 1 equiv) were first suspended in 194 g of basic aqueous solution (4.23 wt % NaOH) for 30 min at room temperature to be swollen and increase the accessibility of hydroxyl groups to chemical reagents. Then, IPA (83 g) was progressively introduced over 30 min. The reaction medium was progressively heated up to 60 °C over 1 h, and propargyl bromide (**2**; 13.78 g, 80 wt % in toluene, 92.65 mmol, 5 equiv) was rapidly added. After reaction at 60 °C, the fibers were filtered and washed with water, IPA, H_2O/IPA (40/60, v/v) mixtures (×3), and finally, with pure water. The obtained product (**3**) was dried at 50−60 °C overnight.

*Preparation of Alkyne-Functionalized Cellulose Fibers (**3**) in Aqueous Process (Reactions **2**−**4**).* Cellulose fibers (**1**; 1.9 g, 11.7 mmol anhydroglucose unit, 1 equiv) were suspended in 200 mL of basic aqueous solution (1.1 wt % NaOH) for 1 h at room temperature to be swollen and increase the accessibility of hydroxyl groups to chemical reagents. The reaction medium was progressively heated up to 60 °C over 1 h. Then, propargyl bromide (**2**; 8.7 g, 80 wt % in toluene, 58.5 mmol, 5 equiv) was quickly added. After reaction at 60 °C, the fibers were filtered and washed with water, IPA, H_2O/IPA (40/60, v/v) mixtures (×3), and finally, with pure water. The obtained product (**3**) was dried at 50−60 °C overnight.

The general conditions of etherification and the characteristics of the resulting materials are given (Table 1).

Table 1. Experimental Conditions of Etherification and Features of the Alkyne-Functionalized Cellulose

reaction	medium w/IPA	$n_{PgBr/AGU}$	NaOH wt %	time/h	DS[a]
1	100/0	3	5.1	24	0.010 ± 0.001
2	100/0	5	1.1	0.5	0.020 ± 0.002
3	100/0	5	1.1	4	0.040 ± 0.004
4	100/0	5	1.1	24	0.060 ± 0.006
5	100/0	5	3.0	0.5	0.030 ± 0.003
6	100/0	5	3.0	4	0.040 ± 0.004
7	100/0	5	3.0	24	0.030 ± 0.003
8	100/0	20	1.1	24	0.050 ± 0.005
9	100/0	20	5.1	24	0.190 ± 0.025
10	70/30	3	5.5	24	0.020 ± 0.002
11	70/30	5	1.1	24	0.080 ± 0.009
12	70/30	5	3.0	0.5	0.050 ± 0.005
13	70/30	5	3.0	4	0.060 ± 0.007
14	70/30	5	3.0	24	0.050 ± 0.005
15	70/30	10	1.1	24	0.090 ± 0.011
16	70/30	20	1.1	24	0.100 ± 0.012
17	20/80[b]	20	1.1	24	0.260 ± 0.035

[a]Determined from elemental analysis. [b]Under these conditions, alteration of the cellulose fibers is observed.

*Preparation of Cellulose Fibers Grafted with 2-Bromopropionic Acid 3-Azido-propyl Ester by CuAAC Coupling (**5**).* The protocol of CuAAC coupling was the same whatever the DS of the alkyne-functionalized fibers (**3**). The quantity of reagents to be incorporated was calculated in regards to the maximal value of DS obtained, that is, 0.26 (reaction **17**). Alkyne-functionalized fibers (**3**; 200 mg, 0.30 mmol of alkyne groups, 1 equiv) were introduced in a solution of H_2O/IPA (50/50 w/w, 8 g). A 9 wt % aqueous sodium ascorbate solution (2.58 g, 1.17 mmol, 3.9 equiv) was added to the solution and the vial was protected with aluminum foil. 2-Bromopropionic acid 3-azido-propyl ester (**4**; 276 mg, 1.17 mmol, 3.9 equiv) was introduced. The reaction was triggered by incorporating a 0.7 wt % aqueous copper sulfate solution (1.33 g, 59 μmol, 0.20 equiv). After 65 h of reaction at ambient temperature, the medium was filtered and washed with water, IPA, chloroform, and water. The grafted fibers (**5**) were finally dried overnight at 50 °C. Similar experiments without addition of copper catalyst were conducted from alkyne-functionalized fibers (**3**) providing a control sample.

*Preparation of Cellulose Fibers Grafted with Azide-Functionalized Alexa Fluor 488 by CuAAC Coupling (**7**).* Alkyne-functionalized fibers (**3**; DS = 0.06, reaction **13**; 1 mg, 0.365 μmol alkyne function, 1 equiv) were introduced in water (2.17 g) at room temperature and stirred for 1 h. A 3.85 wt % aqueous sodium ascorbate solution (6 μL, 1.18 μmol, 3.2 equiv) was then added. The vial was

Scheme 1. General Strategy of Cellulose Fibers Alkynation

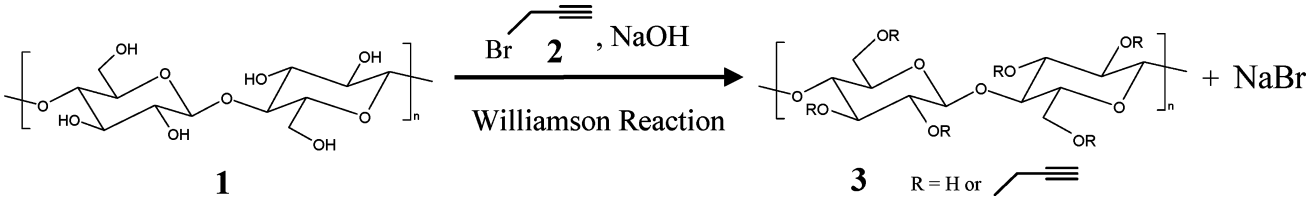

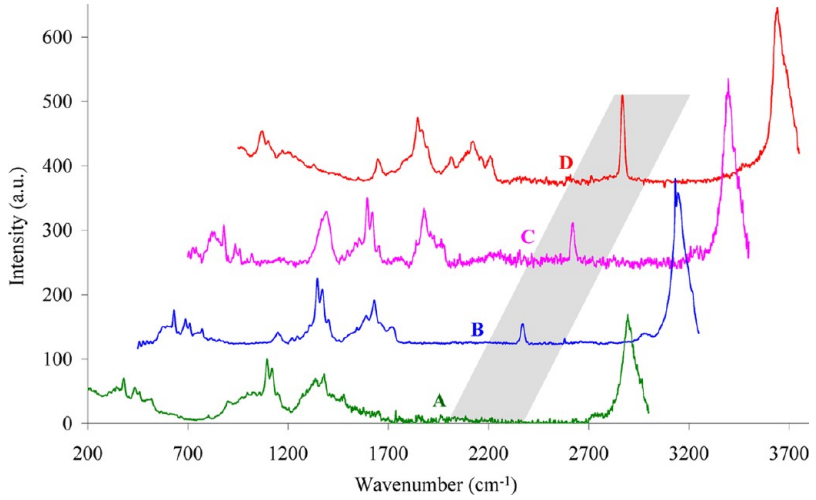

Figure 1. Raman spectra of raw cellulose fibers (curve A) of alkyne-functionalized cellulose fibers generated in water (curve B, reaction **8**) and hydro-alcoholic media (curve C: H_2O/IPA 70/30, reaction **16**; and curve D: H_2O/IPA 20/80, reaction **17**).

protected with aluminum foil and stirred for 1 h. An azide-functionalized Alexa Fluor 488 marker (**6**) in a DMSO solution (1 mg in 639 mg, 1.16 μmol, 3.2 equiv) was introduced in the solution. A total of 3 g of water was used to rinse the Alexa Fluor 488 packaging and added in the medium. Finally, a 0.008 wt % aqueous copper sulfate solution (120 μL, 60 nmol, 0.15 equiv) was added. After 4 h under stirring at ambient temperature, the medium was centrifuged for 5 min at 20 °C. The supernatant was removed and substituted with 5 mL of water. This procedure was repeated six times. The fluorescent Alexa fluor 488-grafted fibers (**7**) were stored in water in the dark. A similar experiment without addition of copper catalyst was performed to provide a control sample.

*Preparation of Cellulose Fibers Grafted with ω-N_3-PEG (M_n = 775 g·mol^{-1}) by CuAAC Coupling (**9**).* In a vial protected from light by aluminum foil, ω-N_3-PEG (**8**; 1.948 g, 2.51 mmol, 7.9 equiv) and 9 wt % aqueous sodium ascorbate solution (1 mL, 0.503 mmol, 1.6 equiv) were added to water (48 mL) at 40 °C. After the solution became homogeneous, alkyne-functionalized fibers (**3**; DS = 0.06, reaction **13**; 0.87 g, 0.317 mmol alkyne functions, 1 equiv) were added. Finally, after 1 h, a 0.4 wt % aqueous copper sulfate solution (1 mL, 25 μmol, 0.08 equiv) was introduced. After 1 day under stirring at 40 °C, the medium was filtered. The grafted fibers were purified (**9**) by Soxhlet extraction (1 day with $CHCl_3$ and 2 days with H_2O) and dried at 50 °C overnight.

RESULTS AND DISCUSSION

Alkyne Functionalization of Wood Cellulose Fibers. The alkynation of the fibers was performed through Williamson etherification (Scheme 1) in the presence of sodium hydroxide and propargyl bromide. Williamson etherification was preferred over other reactions, such as esterification, on account of its water compatibility and the formation of stable ether links. Aiming at identifying experimental conditions allowing for substantial alkyne functionalization of the cellulose fibers without alteration of their integrity, the influence of several experimental parameters, such as the composition of the reaction medium (water or water/IPA mixtures), the sodium hydroxide weight ratio, the propargyl/cellulose hydroxyl groups ratio, and the duration of the reaction, were addressed.

In a preliminary step, the alkyne functionalization of cellulose fibers was investigated in water and water/isopropanol mixtures (70/30 and 20/80 w/w) while keeping the other parameters constant (60 °C, 24 h, $n_{\text{propargyl bromide}}/n_{\text{AGU}}$ = 20/1, 1.1−1.2 wt % NaOH). After extensive rinsing of the fibers (see Experimental Section), progress of the etherification was qualitatively monitored by Raman spectroscopy and FT-IR (Figure 1 and Figure S1 in Supporting Information). As illustrated by Figure 1, the presence of grafted alkyne moieties was evidenced under both aqueous and hydro-alcoholic conditions (100/0, 70/30, and 20/80 w/w, water/IPA) by the appearance of typical C≡C stretching vibrational signals of alkynes at 2120 cm^{-1}. However, notable differences in terms of alkyne incorporation were observed, depending on the IPA content (see Figure 1, curves B−D). It is evident from Figure 1 that the addition of isopropanol as cosolvent promotes the etherification of cellulose. The highest intensities (for the C≡C stretching vibration) are detected when etherification is carried out in isopropanol-rich medium (20/80 w/w, water/IPA), whereas the lowest ones are obtained in aqueous conditions.

As it is crucial to maintain the integrity and the structure of the fibers in the course of the chemical derivatization to preserve the intrinsic features of the cellulose material, the impact of the water/IPA composition (at constant NaOH content) on the crystallinity and the dimensions of the resulting fibers were further investigated. The crystalline structure of raw and alkyne-functionalized cellulose fibers was thus investigated by solid-state ^{13}C CP-MAS NMR spectroscopy[16b] and X-ray

dx.doi.org/10.1021/bm3016829 | Biomacromolecules 2013, 14, 254−263

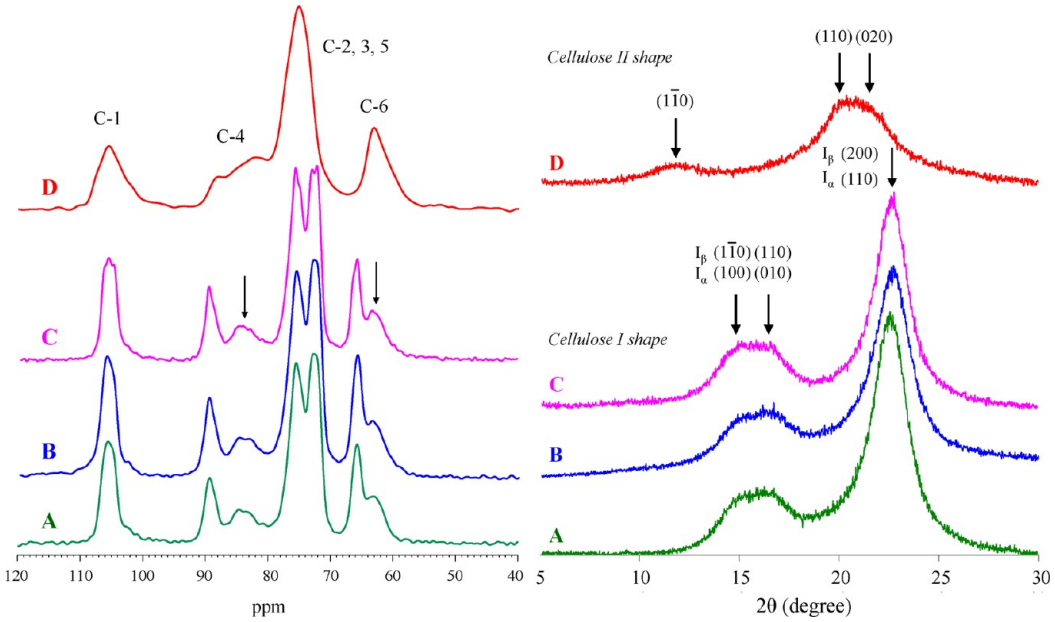

Figure 2. Solid-state ^{13}C CP-MAS NMR spectra (left) and X-ray diffraction patterns (right) of raw cellulose fiber (A), alkyne-functionalized cellulose modified in water (B, reaction **8**) or in hydroalcoholic media H_2O/IPA 70/30 (C, reaction **16**), and in H_2O/IPA 20/80 (D, reaction **17**). On NMR spectra, arrows indicate characteristic broad resonances of amorphous cellulose components. On diffraction patterns, arrows indicate Miller indices for the three principal planes of reflection of cellulose I and cellulose II.

diffraction[18] (Figure 2). Solid-state ^{13}C CP-MAS NMR spectra of raw fibers and alkyne-functionalized cellulose generated in water and in water-rich solutions, that is, 70/30 water/isopropanol (curves B and C) all display the typical patterns of highly crystalline cellulose and the resonance signals arising from carbons belonging to the amorphous zones of the fibers (pointed out by arrows) were identical in terms of shape and intensity suggesting that the structure of the cellulose material is not altered in the course of the alkynation process.

Conversely, the ^{13}C CP-MAS NMR spectrum of alkyne-functionalized cellulose fibers obtained in isopropanol-rich conditions (curve D) is notably distinct. All the peaks are broadened and those originating from amorphous regions are obviously more pronounced[16a] indicating that the isopropanol-rich medium causes major modifications of the crystalline structure of cellulose fibers. These assessments are also supported by the X-ray diffraction patterns of raw and alkyne-functionalized fibers given in Figure 2. Again, no significant difference could be noticed between the diffractograms of raw and alkyne-functionalized fibers generated in water or water-rich conditions (Figure 2, patterns A–C). In both cases, the diffraction patterns display the characteristic Miller indices for the main reflection planes of cellulose I with the existence of two suballomorphs, namely, I_α and I_β.[19] On the contrary, pattern D related to alkyne-functionalized cellulose fibers obtained in isopropanol-rich conditions provides clear evidence that cellulose fibers adopt a modified crystal structure irreversibly forming the cellulose II allomorph.[20] The former behavior was previously described in the case of the preparation of cellulose ether derivatives through isopropyl alcohol–water–sodium hydroxide medium.[21]

The influence of the reaction medium on fibers dimensions was also examined by automated optical analyses on raw cellulose fibers and presuspended fibers in the alcohol and water-rich media used for the etherification. Consistent with the conclusions drawn from NMR and XRD analyses, no noteworthy modification of dimensions could be observed under water-rich and water conditions (respectively, 1840 × 30, 1810 × 29.5, and 1780 × 29 μm for raw cellulose fibers, fibers in water, and water-rich conditions). In contrast, a drastic reduction of the fibers mean length was detected (1490 × 30.5 μm) in the alcohol-rich medium, suggesting that the alteration of the crystalline domains under such conditions impacts the dimensions of the fibers.

The major influence of the isopropanol-rich medium on fibers crytallinity may originate from the demixing of the hydroalcoholic mixture in the range of studied temperatures. This phase separation results in the formation of a weakly sodium hydroxide concentrated alcohol-rich phase and of a strongly sodium hydroxide concentrated aqueous phase prone to migrate within cellulose fibers. This harsh basic treatment probably induces a disruption of intra- and intermolecular hydrogen bonds, ultimately resulting in modifications in crystal structure (similar to mercerization cellulose I → cellulose II) as well as a decrease of the crystallinity index. Moreover, this partial alteration of the crystalline regions in alcohol-rich medium could promote the migration of propargyl bromide within fibers and provide additional hydroxyl sites for alkynation resulting in higher values of DS.

Quantification (and optimization) of the etherification process of cellulose fibers was further investigated under nondegrading water and water-rich conditions. The influence of the PgBr/AGU molar ratio, reaction time and sodium hydroxide (at concentrations that preserve the features of cellulose fibers, see Figure S2 in Supporting Information) on the etherification process was addressed. The conditions of etherification and the degrees of substitution of the resulting fibers deduced from elemental analysis are given in Table 1.

Close inspection of Table 1 enables to evaluate the influence of each parameter on the effectiveness of the etherification. Consistent with our preliminary findings (see Figures 1 and S1), the highest degree of substitution (0.26) is obtained for

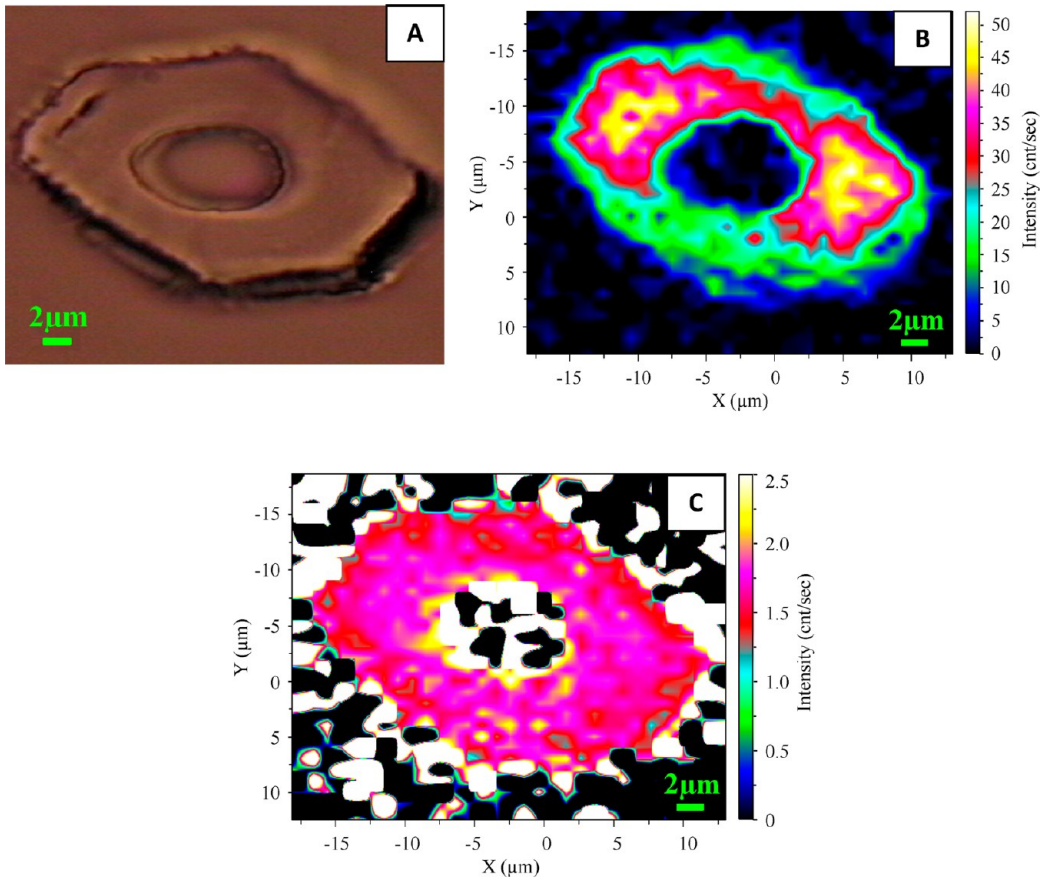

Figure 3. Micrographs of an alkyne-functionalized fiber (reaction **14**) embedded in epoxy resin: optical micrograph (A) and corresponding Raman confocal micrograph (false color) based on the alkyne band intensity at 2120 cm^{-1} (B) or on the 1380/2120 intensity ratio (C).

the etherification in (cellulose-degrading) isopropanol-rich conditions (Table 1, reaction **17**). More generally, regardless of the other parameters, addition of IPA in the medium promotes the etherification of the fibers (see reactions **8**, **16**, and **17**). The incorporation of alkyne moieties is also clearly favored at high PgBr/AGU molar ratio (reactions **1** vs **9** or **11** vs **15** vs **16**). The highest DS values, 0.19 (reaction **9**) and 0.26 (reaction **17**) are indeed obtained for the highest PgBr/AGU ratios. At this point it is worth mentioning that, in regard to the heterogeneous nature of the grafting process, the presence of unavailable hydroxyl moieties in the ordered domains of the fibers[22] and the rather mild conditions of etherification (especially for reactions **1**–**9**), relatively high values of DS are obtained. The influence of sodium hydroxide on the fibers derivatization is far more difficult to unravel and must be discussed in conjunction with the PgBr/AGU molar ratio because on the one hand sodium hydroxide activates the cellulose hydroxyl groups and on the other hand consumes propargyl bromide. Two trends can actually be distinguished depending on the PgBr/AGU molar ratio. At low PgBr/AGU ratio (≤5), the increase of sodium hydroxide content (from 1.1 to 3 or 5.1 wt %) negatively impacts the etherification of the fibers (see reaction **1** and reactions **4** vs **7** or **11** vs **14**). In contrast, it is evident from comparison of reactions **8** vs **9** that, for the highest PgBr/AGU ratio, incorporation of alkyne moieties onto cellulose fibers is favored upon addition of sodium hydroxide.

Last but not least, whereas highest DS values are obtained after 24 h of reaction, cellulose materials displaying substantial DS can be obtained in 30 min under appropriate conditions of etherification (reactions **2**, **5**, and **12**).

Functionalization Mapping. To gain further information on the alkynation of the cellulose fibers under water or water-rich conditions, a precise mapping of the functionalization at the surface and within the fibers was undertaken. Studies devoted to the characterization of grafted molecules/macromolecules distribution on cellulose substrates are extremely scarce and to our knowledge, limited to surface analysis.[23] Relying on a recent work of Sodeoka and co-workers who elegantly exploited the quite intense Raman signals displayed by alkyne groups at 2120 cm^{-1} to visualize the incorporation of alkyne-tagged molecules into living cells through Raman microscopy, we intended to image the distribution of alkyne moieties all over the fibers by Raman confocal microscopy.[24] Etherified cellulose fibers were embedded into epoxy matrices to allow for characterization of the fibers cross sections. Typical optical and scattering Raman images of alkyne-functionalized fibers (generated in water or water-rich conditions) reconstructed from the distribution of Raman signal at 2120 cm^{-1} are given in Figure 3 (and Figure S3 in Supporting Information) .

As can be seen, alkyne functionalities are detected in the entirety of the cellulose material attesting that propargyl bromide is capable of diffusing (and reacting) in the inner parts of the fibers under basic water or water-rich conditions of etherification. Interestingly, important disparities in terms of alkyne concentrations are observed with the presence of alkyne-rich (yellow) regions located in the core of the fiber and less concentrated (green) regions at the periphery of the fiber. In

dx.doi.org/10.1021/bm3016829 | *Biomacromolecules* 2013, 14, 254–263

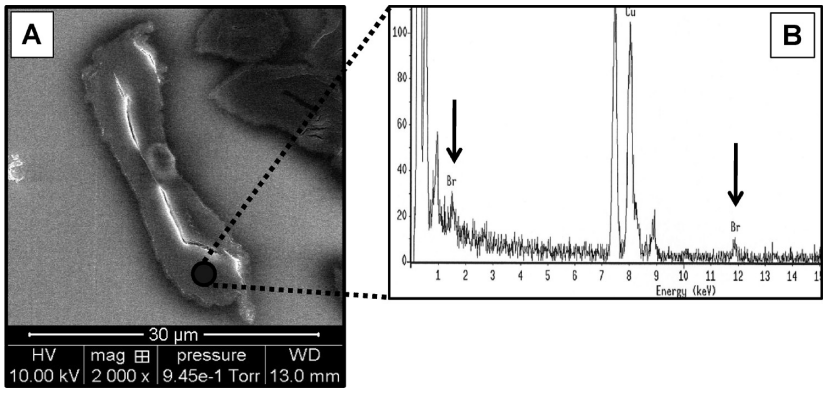

Figure 4. (A) SEM micrograph of (**5**) embedded in epoxy matrix, with the area analyzed by EDX/STEM circled, and (B) EDX spectrum collected on the highlighted area (see arrows relative to Br signals).

Scheme 2. CuAAC Coupling between Alkyne-Functionalized Fiber (3) and Azido Derivatives, 2-Bromopropionic Acid 3-Azido-propyl Ester (4), Alexa fluor 488 Moiety (6), and ω-N_3-PEG (8; M_n = 750 g/mol)

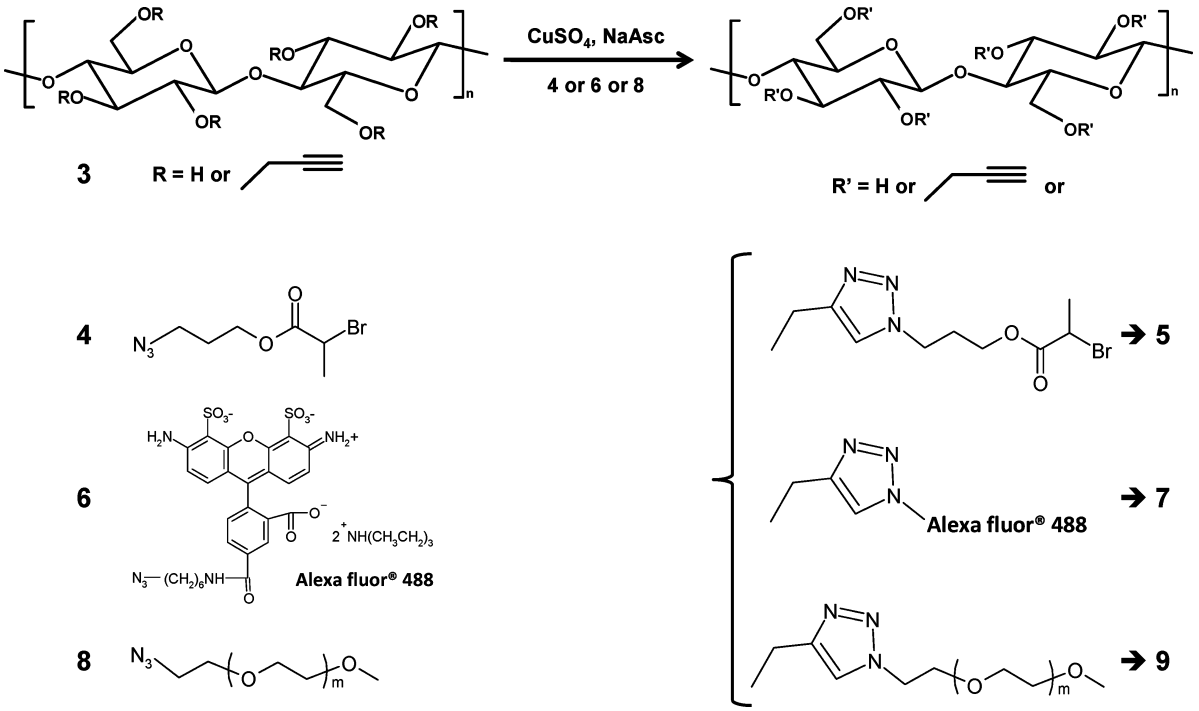

contrast, reconstruction of the images after normalization to a typical band of cellulose backbone at 1380 cm^{-1} (Figure 3C)[25] reveals a homogeneous distribution (of alkyne groups) in the matter, suggesting that etherification is not particularly enhanced inside the fiber. All together, these results rather indicate that the heterogeneous distribution observed in Figure 4 reflects the heterogeneity of the matter density within the cellulose fiber. This gradient of matter density may originate from the final drying step, which could induce aggregation of microfibrils.

The question then arises as to how accessible and reactive are these cellulose-anchored alkyne groups for further modifications of the fibers. In this context, the grafting of a range of azide-functionalized molecular probes or macromolecules (Scheme 2) onto alkyne-functionalized fibers through CuAAC coupling was subsequently explored.

In this view, the CuAAC reaction between alkyne-functionalized fibers and 2-bromopropionic acid 3-azido-propyl ester (**4**) was first examined in water-rich swelling medium at ambient temperature (see Experimental Section). The quantitative character of the "grafting onto" process was clearly evidenced by both FT-IR (not shown) and Raman spectroscopies, where the typical signal of C≡C bonds (at ∼2120 cm^{-1}) was no longer visible after reaction with (**4**; Figure S4, Supporting Information). The absence of residual alkyne moieties was further supported by Raman confocal microscopy (Figure S5, Supporting Information). The success of the conjugation between **3** and **4** was also confirmed by elemental analyses from nitrogen content and EDX/STEM analyses highlighting the presence of the bromide element all over the fiber (see Figure 4).

Further investigations on the "grafting onto process" were carried out with Alexa fluor 488 (**6**), an azide-functionalized fluorescent tag, in order to visualize the distribution of the grafted fluorophore in the fiber through fluorescence confocal microscopy.[7a,12b,26] Figure 5 depicts typical fluorescence

dx.doi.org/10.1021/bm3016829 | Biomacromolecules 2013, 14, 254−263

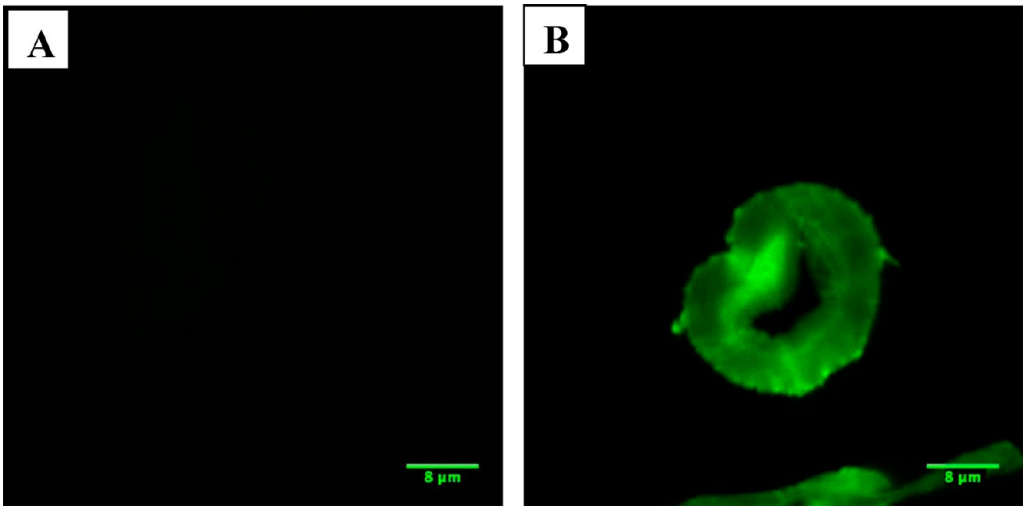

Figure 5. Fluorescence confocal micrographs of cellulose fibers cross sections. (A) Control sample: alkyne-functionalized fiber mixed with (**6**) without catalyst; (B) fiber clicked with (**6**).

confocal microscopic micrographs recorded on a control sample corresponding to fibers exposed to the fluorophore without catalyst addition and fibers clicked with Alexa dye in water-rich swelling medium.

Whereas fibers are not visualized for the blank experiment (Figure 5A), micrograph of the cellulose materials after clicking (Figure 5B) emphasizes the presence of fluorescence tags all over the fiber that confirms the effectiveness of the ligation. Importantly, consistent with the peculiar distribution of the alkyne functions highlighted by Raman confocal microscopy (Figure 3), a gradient of fluorescence (with significantly higher intensities inside the fibers) is observed.

Aiming at generating cellulose-based biohybrids in non-degrading conditions, alkyne-functionalized fibers (**3**) were finally reacted with ω-N_3-PEG (**8**; M_n = 750 g/mol) in water (Scheme 2, derivative **9**). The resulting fibers were subsequently subjected to an intensive washing step through Soxhlet extraction with successively chloroform and water in order to remove any untethered polymers prior to NMR and Raman characterizations. Solid-state ^{13}C SPE-MAS NMR experiments were carried out on raw cellulose fibers, alkyne-functionalized fibers (**3**) and PEG clicked fibers (**9**; Figure 6). By selecting a short recycle delay, ^{13}C SPE-MAS NMR (contrary to ^{13}C CP-MAS) analysis allows for detecting signals from carbons with short relaxation times.[27] Hence, the technique is very sensitive to the resonance to the most mobile segments at the molecular scale and is therefore particularly relevant to discern the signal of flexible polyether grafted on the fibers. The appearance of a peak at 70.5 ppm on the spectrum of clicked cellulose fibers (Figure 6C) unambiguously validated the successful grafting of PEG chains onto the alkyne-functionalized fibers.[17] Importantly, with the exception of the peak at 70.5 ppm, the spectrum of clicked cellulose fibers is very similar to those of alkyne-functionalized fibers and raw cellulose in the 40−120 ppm (Figure 6A,B) confirming that the grafting of the PEG chains does not alter the structure of the cellulose substrate. Congruent conclusions were drawn from solid-state ^1H MAS NMR analysis of raw and modified cellulose fibers (Figure S6, Supporting Information). Note that the triazole rings were too sparse to be detected at 130 and 140 ppm by ^{13}C CP-MAS or ^{13}C SPE-MAS experiments (Figure S7, Supporting Information).

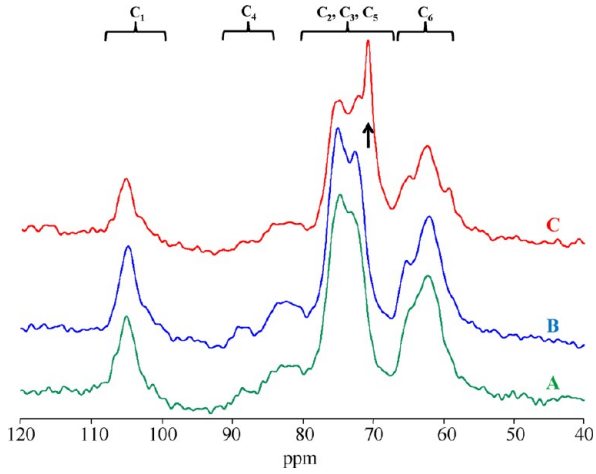

Figure 6. Solid-state ^{13}C SPE-MAS NMR spectra of unmodified cellulose (A), of alkyne-functionalized cellulose (**3**; B), and of PEG-grafted cellulose (**9**; C). The arrow indicates the characteristic signal of grafted PEG and spectra are typical of cellulose I.

Elemental analysis of the resulting biohybrids (based on nitrogen content) allowed for evaluating the efficiency of the PEG-grafting procedure. It was deduced from the calculated DS_{PEG} value (0.02−0.03) that, in contrast with previous grafting procedures involving molecular probes, the CuAAC coupling of macromolecular grafts is not quantitative (30% of converted alkynes). This incomplete functionalization of the cellulose fibers was further corroborated by Raman confocal microscopy (based on the alkyne band intensity at 2120 cm^{-1}), which clearly underpinned the presence of residual unreacted alkyne groups inside the fiber (yellow and pink regions in Figure 7B). In contrast with the ligation of azide-functionalized molecular probes, the grafting of the PEG segments may be hampered by a limited diffusion of the polyether chains within the fibers as well as the potential adsorption of the PEG chains at the surface of the fibers favored by the establishment of hydrogen interactions.

CONCLUSIONS

An original route to alkyne-functionalized wood cellulose fibers under green and nondegrading basic aqueous or hydroalcoholic

dx.doi.org/10.1021/bm3016829 | Biomacromolecules 2013, 14, 254−263

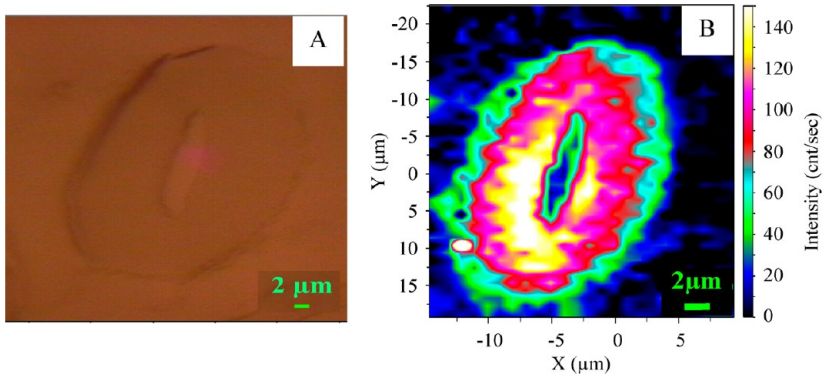

Figure 7. Micrographs of an alkyne-functionalized fiber after grafting with ω-N_3-PEG (**9**): optical micrograph (A) and Raman confocal micrograph (false color) recorded through the intensity of the alkyne band at 2120 cm^{-1} (B).

(H_2O/IPA) heterogeneous conditions has been developed. It was shown that derivatization of the fibers is significantly favored upon addition of IPA, especially for high ratio of water/IPA (20/80). Under such conditions, the reaction is, however, accompanied by drastic modifications of the crystalline structure of cellulose fibers, namely, conversion of cellulose I to cellulose II and substantial decrease of the crystallinity index. Conversely, etherification in water or water-rich media (100/0 or 70/30) results in lower (but significant) degrees of substitution and preserves the integrity and the features of the fibers. Raman confocal microscopy of modified cellulose fibers cross sections based on a characteristic signal at 2120 cm^{-1} demonstrated the incorporation of alkyne functions all over the fibers and gave evidence of a heterogeneous distribution of the alkyne groups with the presence of alkyne-rich domains in the inner part of the fibers. Effective postmodification of the resulting fibers with azide-functionalized molecular probes and azide end-capped PEG through CuAAC confirmed the high reactivity and the full accessibility of the grafted alkyne moieties under suitable conditions

■ ASSOCIATED CONTENT

Supporting Information

FT-IR spectra and X-ray diffraction patterns of raw cellulose fibers and alkyne-functionalized fibers generated in water and hydroalcoholic media; optical and Raman confocal micrographs of alkyne-functionalized fibers; Raman spectra of raw cellulose fibers, alkyne-functionalized cellulose, and 2-bromopropionic acid 3-azido-propyl ester grafted fibers; optical and Raman confocal micrographs of 2-bromopropionic acid 3-azido-propyl ester grafted fibers; solid state ^{1}H MAS NMR spectra of raw cellulose, alkyne-functionalized cellulose and PEG-grafted cellulose; solid-state ^{13}C CP-MAS and ^{13}C SPE-MAS NMR spectra of PEG-grafted cellulose. This material is available free of charge via the Internet at http://pubs.acs.org.

■ AUTHOR INFORMATION

Corresponding Author

*E-mail: aurelia.charlot@insa-lyon.fr; etienne.fleury@insa-lyon.fr. Fax: +33 (0)4 72 43 85 27.

Notes

The authors declare no competing financial interest.

■ ACKNOWLEDGMENTS

The authors acknowledge CTP (Centre Technique du Papier) for financial support, the Service Central d'Analyse Echangeur de Solaize (France) of the Centre National de Recherche Scientifique for elementary analyses and Raman spectroscopy analyses, GSM laboratory (Groupe de Spectroscopie Moléculaire, Institut des Sciences Moléculaires - UMR 5255, Bordeaux) for Raman confocal microscopy analyses. M.G. thanks UWS for the research support funding associated with her Research Lectureship and the UWS College of Health and Science for an infrastructure grant for solid-state NMR equipment.

■ REFERENCES

(1) Pérez, S.; Samain, D. *Adv. Carbohydr. Chem. Biochem.* **2010**, *64*, 25−116.
(2) Aizenshtein, E. M. *Fibre Chemistry* **2011**, *43*, 395−405.
(3) Klemm, D.; Heublein, B.; Fink, H.-P.; Bohn, A. *Angew. Chem., Int. Ed.* **2005**, *44*, 3358−3393.
(4) Faruk, O.; Bledzki, A.; Fink, H.-P.; Sain, M. *Prog. Polym. Sci.* **2012**, *37*, 1552−1596.
(5) (a) Tizzotti, M.; Labeau, M.-P.; Hamaide, T.; Drockenmuller, A.; Charlot, A.; Fleury, E. *J. Polym. Sci., Part A: Polym. Chem.* **2010**, *48*, 2733. (b) Tizzotti, M.; Charlot, A.; Fleury, E.; Stenzel, M.; Bernard, J. *Macromol. Rapid Commun.* **2010**, *31*, 1751−1772.
(6) Roy, D.; Semsarilar, M.; Guthrie, J.; Perrier, S. *Chem. Soc. Rev.* **2009**, *38*, 2046−2064.
(7) (a) Brumer, H., III; Zhou, Q.; Baumann, M. J.; Carlsson, K.; Teeri, T. T. *J. Am. Chem. Soc.* **2004**, *126*, 5715−5721. (b) Gustavsson, M. T.; Persson, P. V.; Iversen, T.; Martinelle, M.; Hult, K.; Teeri, T. T.; Brumer, H., III *Biomacromolecules* **2005**, *6*, 196−203. (c) Zhou, Q.; Greffe, L.; Baumann, M. J.; Malmström, E.; Teeri, T. T.; Brumer, H., III *Macromolecules* **2005**, *38*, 3547−3549. (d) Zhou, Q.; Brumer, H., III; Teeri, T. T. *Macromolecules* **2009**, *42*, 5430−5432. (e) Xu, C.; Spadiut, O.; Araújo, A. C.; Nakhai, A.; Brumer, H., III *ChemSusChem* **2012**, *5*, 661−665.
(8) Filpponen, I.; Kontturi, E.; Nummelin, S.; Rosilo, H.; Kolehmainen, E.; Ikkala, O.; Laine, J. *Biomacromolecules* **2012**, *13*, 736−742.
(9) (a) Zhang, Y.; Wang, G.; Huang, J. *Macromolecules* **2010**, *43*, 10343−10347. (b) Rostovtsev, V. V.; Green, L. G.; Fokin, V. V.; Sharpless, K. B. *Angew. Chem., Int. Ed.* **2002**, *41*, 2596−2599. (c) Tornoe, C. W.; Christensen, C.; Meldal, M. *J. Org. Chem.* **2002**, *67*, 3057−3064. (d) Singh, I.; Zarafshani, Z.; Lutz, J.-F.; Heaney, F. *Macromolecules* **2009**, *42*, 5411−5413. (e) Fairbanks, B. D.; Scott, T. F.; Kloxin, C. J.; Anseth, K. S.; Bowman, C. N. *Macromolecules* **2009**, *42*, 211−217.
(10) (a) Tizzotti, M.; Creuzet, C.; Labeau, M.-P.; Hamaide, T.; Boisson, F.; Drockenmuller, E.; Charlot, A.; Fleury, E. *Macromolecules* **2010**, *43*, 6843−6852. (b) Faugeras, P.-A.; Elchinger, P.-H.; Brouillette, F.; Montplaisir, D.; Zerrouki, R. *Green Chem.* **2012**, *14*, 598−600.

(11) (a) Filpponen, I.; Argyropoulos, D. S. *Biomacromolecules* **2010**, *11*, 1060−1066. (b) Sadeghifar, H.; Filpponen, I.; Clarke, S.; Brougham, D.; Argyropoulos, D. *J. Mater. Sci.* **2011**, *46*, 7344−7355.
(12) (a) Hafrén, J.; Zou, W.; Córdova, A. *Macromol. Rapid Commun.* **2006**, *27*, 1362−1366. (b) Chen, G.; Tao, L.; Mantovani, G.; Ladmiral, V.; Burt, D. P.; Macpherson, J. V.; Haddleton, D. M. *Soft Matter* **2007**, *3*, 732−739.
(13) Quemener, D.; Davis, T. P.; Barner-Kowollik, C.; Stenzel, M. H. *Chem. Commun. (Cambridge, U. K.)* **2006**, *48*, 5051−5053.
(14) Tizzotti, M.; Creuzet, C.; Labeau, M.-P.; Hamaide, T.; Boisson, F.; Drockenmuller, E.; Charlot, A.; Fleury, E. *Macromolecules* **2010**, *43*, 6843−6852.
(15) Morcombe, C. R.; Zilm, K. W. *J. Magn. Reson.* **2003**, *162*, 479−486.
(16) (a) Isogai, A.; Usuda, M.; Kato, T.; Uryu, T.; Atalla, R. H. *Macromolecules* **1989**, *22*, 3168−3172. (b) VanderHart, D. L.; Atalla, R. H. *Macromolecules* **1984**, *17*, 1465−1472.
(17) Wilhelm, M.; Neidhöfer, M.; Spiegel, S.; Spiess, H. W. *Macromol. Chem. Phys.* **1999**, *200*, 2205−2207.
(18) Wada, M.; Okano, T.; Sugiyama, J. *J. Wood Sci.* **2001**, *47*, 124−128.
(19) (a) Nishiyama, Y.; Langan, P.; Chanzy, H. *J. Am. Chem. Soc.* **2002**, *124*, 9074−9082. (b) Nishiyama, Y.; Sugiyama, J.; Chanzy, H.; Langan, P. *J. Am. Chem. Soc.* **2003**, *125*, 14300−14306.
(20) Langan, P.; Nishiyama, Y.; Chanzy, H. *Biomacromolecules* **2001**, *2*, 410−416.
(21) (a) Yokota, H. *J. Appl. Polym. Sci.* **1985**, *30*, 263−277. (b) Baiardo, M.; Frisoni, G.; Scandola, M.; Licciardello, A. *J. Appl. Polym. Sci.* **2002**, *83*, 38−45.
(22) (a) Habibi, Y.; Chanzy, H.; Vignon, M. R. *Cellulose* **2006**, *13*, 679−687. (b) Goussé, C.; Chanzy, H.; Excoffier, G.; Soubeyrand, L.; Fleury, E. *Polymer* **2002**, *43*, 2645−2651.
(23) (a) Goldmann, A. S.; Tisher, T.; Barner, L.; Bruns, M.; Barner-Kowollik, C. *Biomacromolecules* **2011**, *12*, 1137−1145. (b) Hansson, S.; Tischer, T.; Goldmann, A. S.; Carlmark, A.; Barner-Kowollik, C.; Malmstrom, E. *Polym. Chem.* **2012**, *3*, 307−309. (c) Hansson, S.; Trouillet, V.; Tischer, T.; Goldmann, A. S.; Carlmark, A.; Barner-Kowollik, C.; Malmstrom, E. *Biomacromolecules* **2012**, DOI: 10.1021/bm3013132.
(24) Yamakoshi, H.; Dodo, K.; Okada, M.; Ando, J.; Palonpon, A.; Fujita, K.; Kawata, S.; Sodeoka, M. *J. Am. Chem. Soc.* **2011**, *133*, 6102−6105.
(25) (a) Wiley, J. H.; Atalla, R. H. *Carbohydr. Res.* **1987**, *160*, 113−129. (b) Agarwal, U. *Planta* **2006**, *224*, 1141−1153.
(26) (a) Gimåker, M.; Wågberg, L. *Cellulose* **2009**, *16*, 87−101. (b) Horvath, A. T.; Horvath, A. E.; Lindström, T.; Wågberg, L. *Langmuir* **2008**, *24*, 6585−6594.
(27) (a) Bar-Nes, G.; Hall, R.; Sharma, V.; Gaborieau, M.; Lucas, D.; Castignolles, P.; Gilbert, R. G. *Eur. Polym. J.* **2009**, *45*, 3149−3163. (b) Tang, H.; Hills, B. P. *Biomacromolecules* **2003**, *4*, 1269−1276.